ACS Macro Letters

Letter

pubs.acs.org/macroletters

Hybrid Hydrogels Composed of Regularly Assembled Filamentous Viruses and Gold Nanoparticles

Toshiki Sawada,[†] Sungmin Kang,[†] Junji Watanabe,[†] Hisakazu Mihara,[‡] and Takeshi Serizawa*,[†]

[†]Department of Organic and Polymeric Materials, Graduate School of Science and Engineering, Tokyo Institute of Technology, 2-12-1 Ookayama, Meguro-ku, Tokyo 152-8550, Japan

[‡]Department of Bioengineering, Graduate School of Bioscience and Biotechnology, Tokyo Institute of Technology, 4259-B40 Nagatsuta-cho, Midori-ku, Yokohama 226-8501, Japan

Supporting Information

ABSTRACT: Novel hybrid hydrogels composed of tag-peptides (antigens) displaying filamentous viruses and antibody-immobilized gold nanoparticles (GNPs) through specific interactions between the two components were constructed. The strength of the antigen−antibody interactions greatly affected the macroscopic mechanical properties. The phages and the GNPs in the hydrogels formed lyotropic liquid crystals and well-ordered network structures, respectively. It was suggested that the structurally much different components were cooperatively assembled into the highly regular structures through time-dependent cross-linking processes. This hybrid hydrogel of visible and huge components will open attractive opportunities for the science and technology of next-generation soft materials.

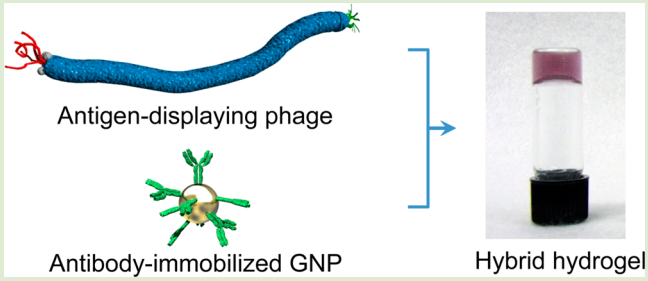

Biomolecular-based assembly engineering is an emerging and highly interdisciplinary field, and biomolecular assemblies are applicable to diverse areas such as electronics, energy, and medical devices.[1−4] Notably, viruses have been developed as candidates for valuable assembling components and are regarded as programmable organic molecules,[3,5,6] because the size and shape of viruses and the number of functional groups on the surfaces are precisely defined by their genomic DNA. In fact, viruses can be modified and functionalized by genetic engineering[7] and synthetic chemical[8,9] methods. Recent studies have clearly revealed that viruses such as filamentous M13 bacteriophages (M13 phages), with a specific affinity for artificial materials or biomolecules, can be utilized to produce batteries and data storage devices,[10−13] sensors,[14] cell-regenerating materials,[15,16] and imaging agents.[17] To widen the applicability of virus-based materials, the control of phage assemblies is an essential requirement.

On the other hand, the efficient and elegant control of nanoparticle assemblies at the nano-to-macro scale via a bottom-up approach is one of the key ambitions of nanoscience and nanotechnology.[18,19] Due to the flexibility of surface modifications and the physicochemical properties derived from quantum size effects, metal nanoparticles with various sizes and shapes attract much attention as assembling components. In particular, gold nanoparticles (GNPs) with unique plasmon properties have been the most frequently investigated as assembling components.[20−22] Among the various assemblies, well-ordered GNPs exhibited unique physical properties, and potentially have a wide range of applications in plasmonics, nanoelectronics, and molecular sensing devices.[21−24] Since their applicability depends greatly on the local order of the GNPs, fundamental methods that can control the assembly states have been developed for utilizing the expressed properties relevant to the assemblies.[18,25]

When M13 phages and GNPs are designed to specifically interact with each other, it is possible to create novel, metal-bioorganic hybrid materials. Those novel hybrid materials would be a promising candidate for the construction and implementation of economically relevant materials that can produce practical bioelectronic, as well as environmental and biomedical tools. In fact, it has been demonstrated that hydrogels composed of genetically engineered highly negative filamentous phages and nanoparticles, in which the two components electrostatically interact with each other, act as a distinguished scaffold for cell culture.[26−28] Here, we constructed hybrid hydrogels composed of M13 phages and GNPs, to which antigen peptides and antibodies were conjugated for specific interactions, respectively. Mixed solutions of the components were transformed into uniform and transparent hydrogels. In the resulting hydrogel assemblies, the M13 phages behaved as liquid crystals and the GNPs formed well-ordered network structures. Both the length of the domain size of liquid crystals and the structured GNPs reached the subcentimeter scale. To the best of our knowledge, this is the first to

Received: February 3, 2014
Accepted: March 19, 2014
Published: March 24, 2014

demonstrate that the cross-linking reactions of filamentous virus termini with spherical nanoparticles cooperatively and effectively regulate the assembled structures of the two heterogeneous components for hybrid hydrogels.

The surfaces of M13 phages and GNPs were modified with antigens and antibodies, respectively, to specifically interact with each other (Figure 1a). Fluorescamine assays demonstrated that 19.7 ± 1.9, 14.5 ± 3.9, and 17.9 ± 2.7 molecules of anti-HA, anti-FLAG, and anti-Myc antibodies were immobilized on each GNP, respectively. Since the number of anti-HA antibodies was slightly greater than that of immobilized Protein A molecules (16 molecules), some of the antibodies seemed to be immobilized by nonspecific physical adsorptions on the GNPs.

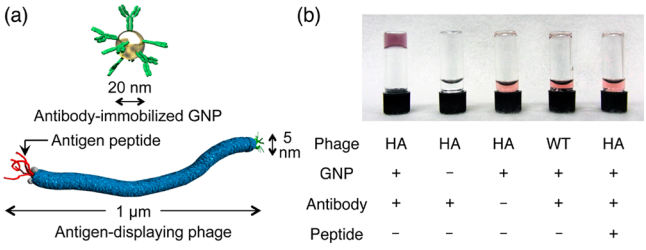

Figure 1. (a) Schematic illustration of the antibody-immobilized GNPs (top) and antigen peptide-displaying M13 phages (bottom). (b) Optical photograph of the mixed solutions. Types of phages, and the presence/absence of GNP, antibody, or HA peptide are shown in the figure.

M13 phages displaying HA peptides (HA-phages) have an affinity constant (K_a) of 1.1×10^9 M^{-1} for its antibody.[29] The mixed solutions of the HA-phages and anti-HA antibody-immobilized GNPs (anti-HA GNPs) were transparent and highly viscous, and behaved as uniform self-supporting hydrogels in the vial inversion test (leftmost in Figure 1b), indicating that the anti-HA GNPs and the HA-phages formed highly networked structures. In contrast, in the absence of the GNPs or the antibodies, or when using wild type (WT) phages (without displayed antigen peptides), the mixed solutions showed much lower viscosity (second, third, and fourth from the left in Figure 1b, respectively), so that the solutions rapidly fell down to the bottom of the vials. Additionally, in the presence of excess amounts of chemically synthesized HA peptides (final concentration: 10 mM), the mixed solution similarly fell down (rightmost in Figure 1b), suggesting that the interactions between antibodies on the GNPs and antigen peptides at the phage termini were inhibited by free antigen peptides. Therefore, these results strongly supported that the specific interactions at phage termini were essential to form hydrogels. In fact, it was reported that biomolecular recognition such as assemblies of coiled-coil peptides[31] and antigen–antibody (Fab fragments) interactions[32] were utilized for responsive capabilities of the hydrogels; therefore, the affinities between antigen peptides on phages and antibodies on GNPs are considered to be sufficient to form hydrogels.

Phages displaying FLAG or Myc peptides and those antibodies were used instead of the HA peptides and the antibodies (FLAG- and Myc-phages, respectively). Although the K_a values of the FLAG- and Myc-phages against those antibodies were smaller than that of the HA-phage (0.19×10^9 and 0.069×10^9 M^{-1}, respectively),[29] hydrogelation was also observed under the same conditions (Figure S1). Accordingly, it was found that specific interactions between the antigen peptides at the phage termini and the antibodies immobilized on the GNPs were generally useful to form network structures in sufficient quantities to greatly increase the viscosity of those solutions. When all the immobilized antibodies are used for interactions with the HA-phages, aggregates would be observed in the mixed solutions. Therefore, suitable amounts of the antibodies on the GNPs seemed to be used for the construction of network structures.

To determine the viscoelastic properties of the hydrogels, rheological studies using frequency-sweep experiments were performed to assess the mechanical properties, the storage modulus (G') and the loss modulus (G''), which represent the elastically stored energy and the energy lost as heat within the hydrogel, respectively. The G' values were greater than the G'' values at all frequencies (Figure S2), indicating that mixtures of the HA-phages and the anti-HA GNPs clearly formed hydrogel. The observed G' value of this virus-GNPs system is comparable to that typically observed for collagen hydrogels[33] and was higher than values for typical hydrogels composed of self-assembling biomolecules such as peptides[34−37] and proteins.[38] These results indicated that novel metal–biomolecular hybrid materials, hydrogels, were constructed successfully.

The mechanical strength of the hydrogels composed of the antigen-displaying phages and the antibody-immobilized GNPs were analyzed quantitatively by a gel indentation hardness test. As a result, rupture forces as a function of the dent distances were obtained (Figure S3). The hydrogels were fractured at the defined distance, whereas the phage solution without antibodies did not exhibit any defined rupture forces. The observed rupture forces of the hydrogels prepared at the different phage and GNP concentrations are summarized in Figure 2 as the hydrogel strength. In the case of HA-phages, increased rupture forces were observed depending on the concentration increase. The concentration dependence of phages against the hydrogel strength was also observed in the case of FLAG- and Myc-phages. This result suggested that well-assembled phages at higher concentrations were effectively entangled to promote the hydrogel strengths. Interestingly, comparing the strengths between the peptide species displayed on phages under the same conditions suggested that the strengths were simply dependent on the K_a values of the phages against antibodies.

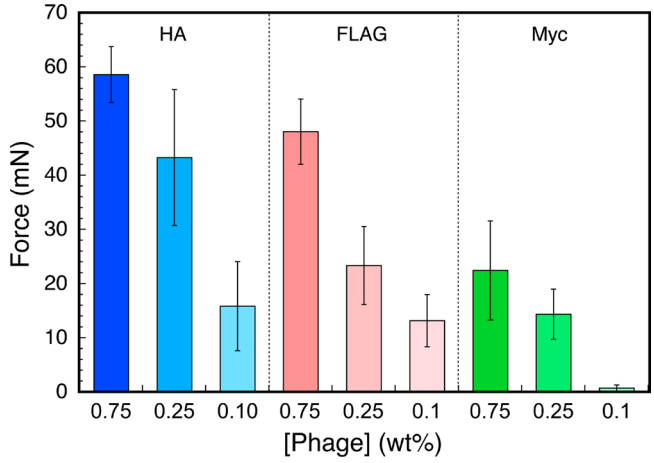

Figure 2. Mechanical strength of the hydrogels. The antigen peptides displayed on the phages and the concentrations are shown. The concentrations of the GNPs were 10 nM.

dx.doi.org/10.1021/mz500073t | ACS Macro Lett. 2014, 3, 341−345

Therefore, molecular-level interactions between peptides at the phage termini and the antibodies on the GNPs were crucial for macroscopic physical properties, such as the mechanical strengths of the hydrogels.

Polarized optical microscopy (POM) observation was performed to investigate the ordered structures of the phages in the hydrogels. Just after mixing the HA-phages and the anti-HA GNPs, an isotropic phase was substantiated (Figure 3a, inset); however, obvious birefringence was identified after 15 min incubation (Figure 3a). Furthermore, the bright domains increased in size with increasing incubation time (up to 30 min) to approximately 100 μm in width (Figure 3b). Since birefringence is generally caused by crystalline particle dispersion or the molecular orientation of solutes,[39] these observations clearly suggest the presence of the highly ordered structures in the hydrogels, of which the domain size reaches the subcentimeter scale. Magnified POM images clearly demonstrated that the bright domains were darkened, while the dark domains were brightened by every 45° rotation of the hydrogels (Figure 3c,d), suggesting the formation of lyotropic liquid crystals. It has been reported that M13 phages alone form lyotropic liquid crystals in aqueous suspension.[40] However, the concentration of phages in this study was 3 times lower than that typically required for liquid crystal formation.[3,40] Therefore, the cross-linking reactions of the HA-phage termini with the anti-HA GNPs successfully induced liquid crystal formation of the HA-phages, as well as simultaneous network structure formation of the anti-HA GNPs. Note that both the HA-phage solutions without the anti-HA GNPs and the mixed solutions of the HA-phages and GNPs without antibodies did not show any birefringence (Figure S4). Taking all the POM observations together, we concluded that the HA-phages were in three-dimensionally highly ordered states by assembling with the anti-HA GNPs.

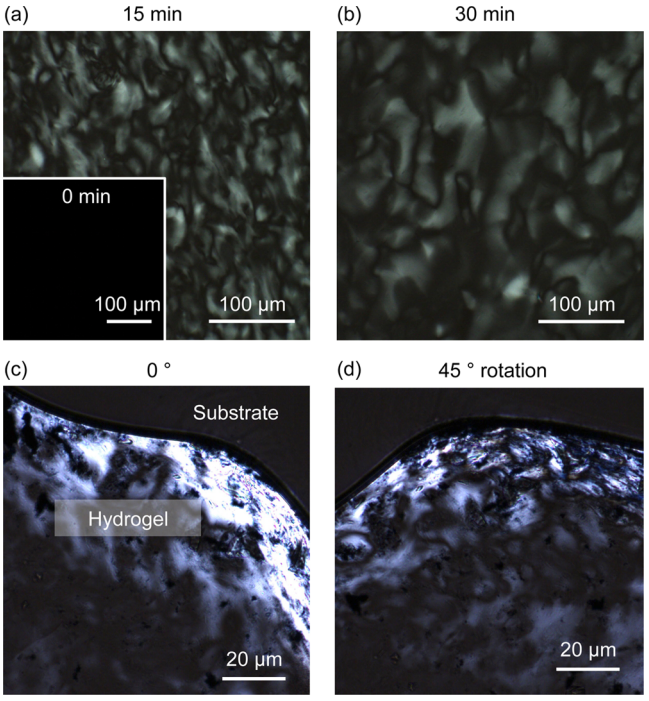

Figure 3. POM images of the hydrogels. (a, b) Time-dependent POM images for the assembly process of the HA-phages and the anti-HA GNPs. (c, d) Magnified POM images after a 45° rotation of the hydrogel.

Transmission electron microscopy (TEM) observation was performed by transferring the hydrogel to a collodion coated copper EM grid, to investigate the ordered structures of the GNPs in the hydrogels. In the TEM image, well-ordered network structures, several tens of micrometers long, were observed (Figure 4a). High magnification images clearly showed that the ordered structures were composed of GNPs (Figure S5a,b). Interestingly, the branched side chains tended to proceed perpendicularly from the main chains in a self-similar manner. Note that the main chains reached the subcentimeter size when followed on the TEM grid. In contrast, using WT phages, ordered structures of GNPs were not observed (Figure S5c). Therefore, specific interactions were necessary to construct the highly regular mesoscale structures. In a previous study, hydrogels composed of positively charged GNPs and negatively charged M13 phages were prepared through electrostatic interactions;[26−28] however, the fine assembly structures of the component GNPs were not investigated microscopically.

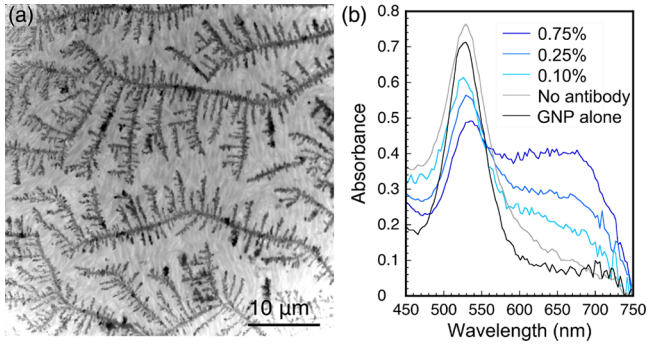

Figure 4. Characterization of ordered structures of GNPs in the hydrogels. (a) TEM image of the well-ordered network GNPs in the hydrogel. (b) Absorption spectra of the anti-HA GNPs with and without the HA-phages, and unmodified GNPs with the HA-phages (0.75%). The concentrations of the HA-phages are shown in the figure.

Absorption spectroscopy analyses were performed to characterize the plasmonic interactions between the GNPs in the hydrogels. The absorption spectra of the anti-HA GNPs with and without the HA-phages after 30 min incubation are shown in Figure 4b. The spectrum of the anti-HA GNPs alone showed a single sharp band at 525 nm (Figure 4b, black line). It has been reported that solutions of well-dispersed GNPs with a diameter of 20 nm showed a λ_{max} at 525 nm;[41] therefore, the anti-HA GNPs were in well dispersed states. In marked contrast, a reduction in the intensity of the 525 nm bands, as well as a broad new absorption band from 600 to 750 nm, was observed after the interaction with the 0.10% HA-phages (Figure 4b, light blue line). Note that the change in absorption spectra was completed within a couple of minutes after mixing the anti-HA GNPs with the HA-phages. Increasing the HA-phage concentration further decreased the intensity of the 525 nm band, and increased the intensity of the additional broad band (Figure 4b, blue and dark blue lines at the 0.25 and 0.75% HA-phage concentrations, respectively). Importantly, the band at 525 nm apparently demonstrating dispersion remained even at high phage concentrations, possibly suggesting that the anti-HA GNPs formed well-ordered 1-D like structures.[23,42] When

dx.doi.org/10.1021/mz500073t | ACS Macro Lett. 2014, 3, 341−345

the HA-phages and GNPs without antibodies were employed as controls, the additional band did not appear (Figure 4b, gray line). These results strongly suggested that specific antigen−antibody interactions as well as sufficient phage concentrations were essential for the unique spectra derived from the assembled GNPs with the HA-phages in the hydrogels.

It is important to discuss the assembly process of the hydrogels with highly regular structures composed of liquid crystalline M13 phages and well-ordered GNPs. As described in the POM observations and absorption spectra, the time required for assembly was in the order of several tens of minutes. Taking into account the huge size of the M13 phages (diameter: 6.5 nm; length: 900 nm; molecular weight: 16.3 MDa)[43] and the position of antigen peptides displayed at the phage termini, it is hard to accept that the assembly of "monodispersed" phages with GNPs proceeded within the time. On the contrary, since the phage concentration used in this study is close to that required for liquid crystal formation,[3] it must be reasonable to consider that the anti-HA GNPs bind to cross-link preordered, but non liquid crystalline HA-phages, followed by time-dependent structural development to regular assemblies of the two heterogeneous components in a cooperative manner for construction of the hydrogels (Figure S6).

In conclusion, we investigated the assembly between antigen peptide-displaying filamentous phages and antibody-immobilized GNPs based on specific interactions. The mixed solutions developed to uniform and transparent hydrogels, indicating that the two components formed highly networked structures at the macroscopic level. The assembly structures of phages and GNPs were successfully analyzed based on their characteristic physicochemical properties. It was therefore revealed that the assembled hydrogels were composed of liquid crystalline phages and well-ordered network structures of GNPs, indicating that both components were cooperatively assembled into the highly regular mesoscale structures. Since phages can be functionalized biotechnologically with the desired peptide or protein, and chemically with unnatural molecules, various functions can be endowed to the novel hybrid hydrogels in the near future. Furthermore, other inorganic and organic nanoparticles can also be constituents in the unique hydrogels. These applications will unlock novel and imaginative opportunities for the exploitation of next-generation self-assembling soft materials composed of regularly ordered structures.

■ MATERIALS AND METHODS

Materials: Ph.D. Peptide Display Cloning System, antitag peptide antibodies (mouse IgG1), and Protein A-conjugated GNPs (Lot: 12353) with a diameter of 20 nm were purchased from New England Biolabs, Inc., Sigma-Aldrich, and BBI solutions, respectively. All other reagents were purchased from Nacalai Tesque. Ultrapure water with more than 18.2 MΩ·cm was supplied by the Milli-Q system (Merck Millipore) and was used throughout all the experiments.

Preparation of antigen peptide-displaying phages: HA (sequence: YPYDVPDYA), FLAG (sequence: DYKDDDDK), and Myc (sequence: EQKLISEEDL) peptides were genetically fused to the pIII minor coat proteins of the M13 bacteriophage via Gly-Gly-Gly-Ser as a spacer using the Ph.D. Peptide Display Cloning System. The constructed phagemid vector was heat-shocked into competent *Escherichia coli* (*E. coli*) ER2738 cells, and amplified. Then, the expressed phages were purified by precipitation and redispersion procedures in the presence of PEG and NaCl. Each phage displayed plural (from 3 to 5) copies of antigen peptides. The correct construction was confirmed by DNA sequencing and enzyme-linked immunosorbent assays method previously described.[29]

Preparation of antibody-immobilized GNPs and construction of hybrid hydrogels: Antibodies for tag peptides and Protein A-conjugated GNPs (16 Protein A molecules were immobilized on the GNP, according to the supplier, which was determined by quantification of unbound Protein A molecules after immobilization) were mixed and incubated for 1 h, thus, preparing the antibody-immobilized GNPs. Unbound antibodies were removed by centrifugation and redispersion procedures. The amounts of unbound antibodies were quantified to determine the amounts of antibodies immobilized on the GNPs using fluorescamine assays, which can estimate the number of exposed amino groups.[30] The antigen phages and the GNPs were mixed in Tris-buffered saline (TBS, 50 mM Tris, 150 mM NaCl, pH 7.5), and the resulting mixture was incubated for 1 h at 20 °C. The concentrations of the phages were set to 0.10, 0.25, and 0.75 wt % (0.10 wt % ≈ 60 nM). The concentration of the GNPs was set to 10 nM.

Absorption measurements: Absorption spectra were recorded on NanoDrop 2000c (Thermo Scientific). Mixed solution of the phages and GNPs were incubated for 30 min. A fraction of the hydrogels (with antibodies) or an aliquot of the mixture (without antibodies) was placed onto the measurement stage and, then, the spectra were recorded.

Rheological studies of the hydrogels: Rheological characterization of the hydrogels was performed by using an Air-Servo mini (Shimadzu). The hydrogel composed of the HA-phages and the anti-HA GNPs with volume of 15 mL was placed on a parallel plate for the rheological test. The concentrations of phages and GNPs were set to 0.75 wt % and 10 nM, respectively. The hydrogel was compressed to measure the G' and the G'' by a frequency-sweeping mode with a fixed strain of 1%.

Indentation test of the hydrogels: The gel strengths were quantitatively investigated by an indentation test using an AGS-X (Shimadzu). A test bar with a diameter of 3 mm was dented into 200 μL of the hydrogels at 1 mm/min, and the forces exerted onto the test bar were monitored in real-time. The hydrogels failed mechanically at distinct dent distances, and these failure points were defined as rupture forces. These rupture forces were defined as the gel strengths.

TEM observation: A collodion-coated copper EM grid was placed coated-side down onto the hydrogels for 30 min, and then the grid was floated onto a droplet of ultrapure water for 1 min. The grid was blotted and then allowed to dry gradually at ambient temperature overnight. All images were taken using a Hitachi H-7500 electron microscope operating at 80 kV.

POM observation: A mixed solution of the HA-phages and the anti-HA GNPs was mounted onto a glass slide, and a cover glass with a gap (height of 20 μm, Matsunami Glass) was gently placed onto the sample. Immediately, the sample was observed by time-dependent POM using an U-AN360P (Olympus) at ambient temperature. After 30 min, high magnification images of the hydrogel were taken, rotating the sample 45° for each image at ambient temperature.

■ ASSOCIATED CONTENT

Ⓢ Supporting Information

Optical photographs, rheological analyses, quantitative gel indentation test, POM images, and TEM images. This material is available free of charge via the Internet at http://pubs.acs.org.

■ AUTHOR INFORMATION

Corresponding Author

*E-mail: serizawa@polymer.titech.ac.jp.

Notes

The authors declare no competing financial interest.

■ ACKNOWLEDGMENTS

This work was supported in part by a Grant-in-Aid for Young Scientists (B) from the Japan Society for the Promotion of

Science (JSPS) (no. 11019204), a Grant for Basic Science Research Project from The Sumitomo Foundation (no. 110427), The Asahi Glass Foundation, The Japan Prize Foundation, and the Mizuho Foundation for the Promotion of Science.

REFERENCES

(1) Zhang, S. *Nat. Biotechnol.* **2003**, *21*, 1171−1178.
(2) Stupp, S. *Nano Lett.* **2010**, *10*, 4783−4786.
(3) Yang, S.; Chung, W.-J.; McFarland, S.; Lee, S.-W. *Chem. Rec.* **2013**, *13*, 43−59.
(4) Ariga, K.; Ji, Q.; Mori, T.; Naito, M.; Yamauchi, Y.; Abe, H.; Hill, J. *Chem. Soc. Rev.* **2013**, *42*, 6322−6345.
(5) Pokorski, J. K.; Steinmetz, N. F. *Mol. Pharmaceutics* **2010**, *8*, 29−43.
(6) Rakonjac, J.; Bennett, N. J.; Spagnuolo, J.; Gagic, D.; Russel, M. *Curr. Issues Mol. Biol.* **2011**, *13*, 51−76.
(7) Smith, G. P.; Petrenko, V. A. *Chem. Rev.* **1997**, *97*, 391−410.
(8) Steinmetz, N.; Bize, A.; Findlay, K. *Adv. Funct. Mater.* **2008**, *18*, 3478−3486.
(9) Joo, K.-I.; Lei, Y.; Lee, C.-L.; Lo, J.; Xie, J.; Hamm-Alvarez, S. F.; Wang, P. *ACS Nano* **2008**, *2*, 1553−1562.
(10) Nam, K. T.; Kim, D.-W.; Yoo, P. J.; Chiang, C.-Y.; Meethong, N.; Hammond, P. T.; Chiang, Y.-M.; Belcher, A. M. *Science* **2006**, *312*, 885−888.
(11) Nam, K. T.; Wartena, R.; Yoo, P. J.; Liau, F. W.; Lee, Y. J.; Chiang, Y.-M.; Hammond, P. T.; Belcher, A. M. *Proc. Natl. Acad. Sci. U.S.A.* **2008**, *105*, 17227−17231.
(12) Lee, Y. J.; Yi, H.; Kim, W.-J.; Kang, K.; Yun, D. S.; Strano, M. S.; Ceder, G.; Belcher, A. M. *Science* **2009**, *324*, 1051−1055.
(13) Dang, X.; Yi, H.; Ham, M.-H.; Qi, J.; Yun, D.; Ladewski, R.; Strano, M.; Hammond, P.; Belcher, A. M. *Nat. Nanotechnol.* **2011**, *6*, 377−461.
(14) Oh, J.-W.; Chung, W.-J.; Heo, K.; Jin, H.-E.; Lee, B.; Wang, E.; Zueger, C.; Wong, W.; Meyer, J.; Kim, C.; Lee, S.-Y.; Kim, W.-G.; Zemla, M.; Auer, M.; Hexemer, A.; Lee, S.-W. *Nat. Commun.* **2014**, *5*, 3043.
(15) Merzlyak, A.; Indrakanti, S.; Lee, S.-W. *Nano Lett.* **2009**, *9*, 846−852.
(16) Chung, W.-J.; Merzlyak, A.; Yoo, S. Y.; Lee, S.-W. *Langmuir* **2010**, *26*, 9885−9890.
(17) Deutscher, S. L. *Chem. Rev.* **2010**, *110*, 3196−3211.
(18) Shaw, C. P.; Fernig, D. G.; Levy, R. *J. Mater. Chem.* **2011**, *21*, 12181−12187.
(19) Alkilany, A.; Lohse, S.; Murphy, C. *Acc. Chem. Res.* **2012**, *46*, 650−661.
(20) Ghosh, S. K.; Pal, T. *Chem. Rev.* **2007**, *107*, 4797−4862.
(21) Wilson, R. *Chem. Soc. Rev.* **2008**, *37*, 2028−2045.
(22) Ding, M.; Sorescu, D.; Kotchey, G.; Star, A. *J. Am. Chem. Soc.* **2012**, *134*, 3472−3479.
(23) Sardar, R.; Shumaker-Parry, J. S. *Nano Lett.* **2008**, *8*, 731−736.
(24) Chen, C.-L.; Rosi, N. L. *J. Am. Chem. Soc.* **2010**, *132*, 6902−6903.
(25) Mandal, S.; Shundo, A.; Acharya, S.; Hill, J.; Ji, Q.; Ariga, K. *Chem. Asian J.* **2009**, *4*, 1055−1058.
(26) Souza, G.; Christianson, D.; Staquicini, F.; Ozawa, M.; Snyder, E.; Sidman, R.; Miller, J.; Arap, W.; Pasqualini, R. *Proc. Natl. Acad. Sci. U.S.A.* **2006**, *103*, 1215−1220.
(27) Souza, G.; Yonel-Gumruk, E.; Fan, D.; Easley, J.; Rangel, R.; Guzman-Rojas, L.; Miller, J.; Arap, W.; Pasqualini, R. *PLoS One* **2008**, *3*, e2242.
(28) Souza, G.; Molina, J.; Raphael, R.; Ozawa, M.; Stark, D.; Levin, C.; Bronk, L.; Ananta, J.; Mandelin, J.; Georgescu, M.-M.; Bankson, J.; Gelovani, J.; Killian, T.; Arap, W.; Pasqualini, R. *Nat. Nanotechnol.* **2010**, *5*, 291−297.
(29) Sawada, T.; Ishiguro, K.; Takahashi, T.; Mihara, H. *Chem. Lett.* **2011**, *40*, 508−509.
(30) Weigele, M.; Blount, J. F.; Tengi, J. P.; Czajkowski, R. C.; Leimgruber, W. *J. Am. Chem. Soc.* **1972**, *94*, 4052−4054.
(31) Tang, A.; Wang, C.; Stewart, R.; Kopeček, J. *J. Controlled Release* **2001**, *72*, 57−70.
(32) Lu, Z.-R.; Kopečková, P.; Kopeček, J. *Macromol. Biosci.* **2003**, *3*, 296−300.
(33) Yang, Y.-l.; Leone, L. M.; Kaufman, L. J. *Biophys. J.* **2009**, *97*, 2051−2060.
(34) Zhang, S. G.; Holmes, T. C.; Dipersio, C. M.; Hynes, R. O.; Su, X.; Rich, A. *Biomaterials* **1995**, *16*, 1385−1393.
(35) Lamm, M. S.; Rajagopal, K.; Schneider, J. P.; Pochan, D. J. *J. Am. Chem. Soc.* **2005**, *127*, 16692−16700.
(36) Yokoi, H.; Kinoshita, T.; Zhang, S. G. *Proc. Natl. Acad. Sci. U.S.A.* **2005**, *102*, 8414−8419.
(37) Aulisa, L.; Dong, H.; Hartgerink, J. D. *Biomacromolecules* **2009**, *10*, 2694−2698.
(38) Mosiewicz, K. A.; Johnsson, K.; Lutolf, M. P. *J. Am. Chem. Soc.* **2010**, *132*, 5972−5974.
(39) Okajima, M.; Kaneko, D.; Mitsumata, T.; Kaneko, T.; Watanabe, J. *Macromolecules* **2009**, *42*, 3057−3062.
(40) Dogic, Z.; Fraden, S. *Curr. Opin. Colloid Interface Sci.* **2006**, *11*, 47−55.
(41) Liu, X.; Atwater, M.; Wang, J.; Huo, Q. *Colloids Surf., B* **2007**, *58*, 3−7.
(42) Lin, S.; Li, M.; Dujardin, E.; Girard, C.; Mann, S. *Adv. Mater.* **2005**, *17*, 2553−2559.
(43) Barbas, C. F.; Burton, D. R.; Scott, J. K.; Silverman, G. J. *Phage Display: A Laboratory Manual*; Cold Spring Harbor Press: New York, 2001.